Crimson Publishers
Wings to the Research

Research Article

Numerical Performance Analysis of an Environment Friendly High Efficiency Copper Based Perovskite Solar Cell Using SCAPS-1D Software

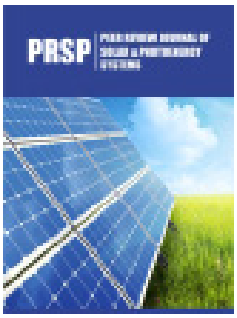

Sunirmal KB*, Monira KM and Shahariar HR

Department of Electrical and Electronic Engineering, Prime University, Bangladesh

***Corresponding author:** Sunirmal Kumar Biswas, Department of Electrical and Electronic Engineering, Prime University, 114/116 Mazar Road, Mipur-1, Dhaka, Bangladesh

Submission: April 16, 2026

Published: May 19, 2026

Volume 3 - Issue 1

How to cite this article: Sunirmal KB*, Monira KM and Shahariar HR. Numerical Performance Analysis of an Environment Friendly High Efficiency Copper Based Perovskite Solar Cell Using SCAPS-1D Software. Peer Rev J Sol Photoen Sys. 3(1). PRSP. 000553. 2026.

Abstract

In this research, we looked at the possibility of using hybrid organic-inorganic material (CH3NH3)2CuCl4 as a material for the absorber in Perovskite Solar Cells (PSCs). Perovskite solar cells are becoming more popular as a possible boost to traditional photovoltaic cells' efficiency. The advantages of this cell over commercial silicon or other organic and inorganic solar cells are its high efficiency and eco-friendliness. In this study, we applied SCAPS-1D software to improve the device performance parameters, using ZnSe as the electron transport layer and $SrCu_2O_2$, which has been identified as a promising photovoltaic hole transport material in the $(CH_3NH_3)_2CuCl_4$-based Perovskite Solar Cell (PSC). To further enhance device performance, we have analyzed the effects of absorber and buffer layer thickness, acceptor density, absorber defect density and interfacial defect densities at the ETL/Absorber and Absorber/HTL interfaces. In addition, we also analyzed the effects of operating temperature, series resistance, and shunt resistance on the Quantum Efficiency (Q-E), back contact materials, current density-voltage (J-V) and overall optimum device performance. Gold is utilized for back contact. The efficient perovskite solar cell achieved an exceptionally high efficiency of 28.5% when the buffer layer was 0.05μm thick and the Absorber layer was 0.6μm thickness.

Introduction

Scientists have been studying alternative energies for decades, since fossil fuels are dirty and finite. We will inevitably look for other energy sources. Fossil fuel sources are getting harder to come by. Consequently, the focus of scientific inquiry has shifted to sustainable energy, with solar energy continuing to be the primary source. Directly converting solar radiation into electrical power is harnessing solar energy [1,2]. The development of third-generation thin film Photo Voltaic (PV) technology has given rise to Perovskite Solar Cells (PSCs). Perovskite solar cells. Have mechanical, optical and physical characteristics that make them appropriate for photovoltaic systems. Scholars have examined some of these attributes through density functional theory and first-principles computation. [3-6]. Double or stacked perovskites are the most promising method for creating lead-free PSCs. This technique substitutes one monovalent M^+ cation and one trivalent M^{2+} cation for the traditional two divalent Pb cations inside the perovskite structure. Consequently, these double perovskites have the following chemical structure: $A_2M+M_2+X_6$, where A can be $CH(NH_2)$ or CH_3NH_{3+} [7]. With its creative structural design, ecologically friendly PSCs could be produced without sacrificing functionality, providing a more sustainable and clean method of solar energy harvesting. We used ZnSe as a buffer layer because ZnSe low cost, high optical transparency, which improves overall device efficiency [8]. With a broad 2.7eV bandgap, ZnSe is a significant technical optoelectronic semiconductor. ZnSe is a suitable replacement for solar photovoltaic cells. It is regarded as a crucial technical material because of its potential uses in various optical and electrical devices and as a buffer and window material for thin-film heterojunction solar cells [9]. This study used $SrCu_2O_2$ as a buffer layer because oxides are more chemically stable

and less moisture sensitive than many organics or halide materials. Using $SrCu_2O_2$ may improve device stability, particularly in operational/ambient exposure. For SCAPS modelling, this supports choosing buffer parameters with less drift (stable defect densities, lifetimes) and exploring stability under temperature variation [10]. It has been discovered that inorganic p-type transparent conductive oxides (TCOs), such as $SrCu_2O_2$, are excellent choices for a hole conductor in solar cells with suitable valence and conduction band locations [11-14]. The proposed pervoskite solar cell used $(CH_3NH_3)_2CuCl_4$ as an absorber layer for Lead-free, lower toxicity, replacing Pb with Cu makes $(CH_3NH_3)_2CuCl_4$ an attractive, environmentally friendlier absorber for lead-free perovskite device concepts, which is an important design consideration in simulation studies where you want to explore non-toxic alternatives [15]. And also used ITO as an ETL layer because it has a realistic bandgap of ITO (~3.5-4.0 eV), so it doesn't absorb visible light significantly [16]. In this simulation, we introduce an ITO/ZnSe/ $(CH_3NH_3)_2CuCl_4$ / $SrCu_2O_2$/Au perovskite solar cell. During this simulation, a total efficiency of 28.5% was gained. This perovskite solar cell can be used for its high efficiency.

Numerical Simulation and Parameters of Materials

The computational model's framework enables an understanding of the fundamentals of solar cells and the key parameters influencing their performance. Crucial one-dimensional semiconductor equations can be solved directly through the SCAPS-1D software [17]. The continuity equations for electrons and holes are as follows:

$$-\left(\frac{1}{q}\right)\frac{d_{jn}}{dX}-U_n+G=\frac{d_n}{dt} \quad (1)$$

$$-\left(\frac{1}{q}\right)\frac{d_{jp}}{dX}-U_p+G=\frac{d_p}{dt} \quad (2)$$

Where J_n and j_p are electrons and hole current densities and G is the generation rate. The Poisson equation is

$$\frac{d^2}{dx^2}T(X)=\frac{e}{\in_0\in_r}(\rho(X)+N_D-N_A+\rho_P-\rho_n \quad (3)$$

The electrostatic potential is represented by ψ, the electrical charge is represented by e, the relative and vacuum permittivity by ε_r and ε_0, the concentrations of holes and electrons are represented by p and n, respectively, the charge impurities of the acceptor and donor types are represented by N_A and N_D, and the distributions of holes and electrons are represented by ρ_p and ρ_n [18]. The literature and the user manual for SCAPS, a very potent program for solar cell performance, provide descriptions of the program and the algorithms it employs [19-22]. For this $(CH_3NH_3)_2CuCl_4$ based Perovskite solar cell Figure 1 displays the schematic diagram (Figure 2) (Table 1).

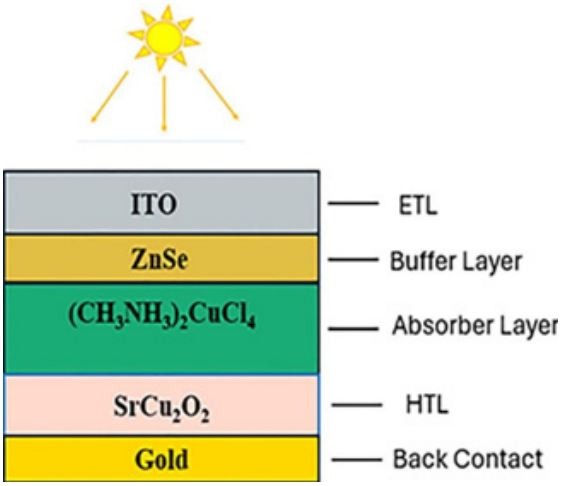

Figure 1: Schematic diagram of proposed perovskite solar cell's schematic diagram.

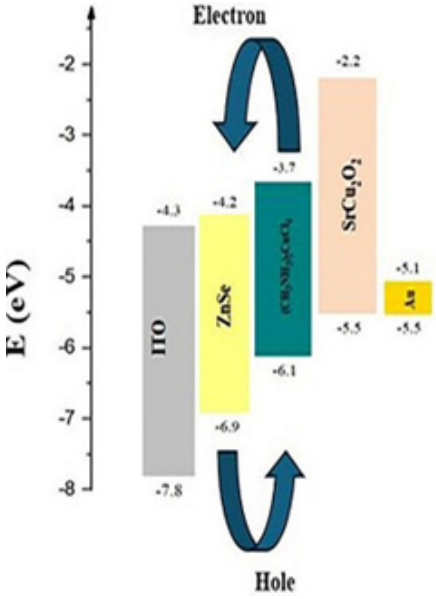

Figure 2: Energy band alignment for various materials utilized in proposed Perovskite solar cell structure.

Table 1: For simulation the materials parameters used in proposed solar cell simulation.

Material Parameter	ITO [41]	ZnSe [9]	$(CH_3NH_3)_2CuCl_4$ [15]	$SrCu_2O_2$[10]
Thickness (μm)	0.1	0.05	0.6	0.2
Band gap (eV)	3.5	2.9	1.2	3.3
Electron affinity (eV)	4	4.1	4.17	2.2
Dielectric permittivity (relative)	9	10	10	9.7
CB effective Density (cm^{-3})	$2.2x10^{18}$	$1.5 x10^{18}$	$2 x10^{18}$	$2 x10^{20}$
VB effective Density (cm^{-3})	$1.8 x10^{19}$	$1.8 x10^{19}$	$1.8 x10^{18}$	$2 x10^{21}$
Electron thermal velocity (cm/s)	10^7	10^7	10^7	10^7

Hole thermal velocity (cm/s)	10^7	10^7	10^7	10^7
Electron mobility (cm^2/V-s)	20	50	3	0.1
Hole mobility (cm^2/V-s)	100	20	1	0.46
Donor density ND (cm^{-3})	1 x10^{21}	1 x10^{18}	0	0
Acceptor density NA (cm^{-3})	0	0	1 x10^{18}	1 x10^{17}
Total Defect Density (cm^{-3})	1 x10^{14}	1 x10^{13}	1 x10^{15}	1 x10^{15}

Results and Discussions

Effect of absorber layer thickness & buffer layer thickness

The thickness of the absorber layer is a significant factor in establishing the device's specifications. The absorber layer thickness on the Perovskite Solar Cell (PSC) is depicted in Figure 3a. The thickness of the absorber layer varies from 0.2µm to 2µm. Figure 3a shows that all solar cell performance parameters, such as Open Circuit Voltage (Voc), Short Circuit Current (Isc), Fil Factor (FF) and efficiency, have improved. Efficiency increases from 22.8% to 28.5%, Isc from 24.62 mA/cm^2 to 34.76mA/cm^2, and FF from 85.05% to 85.5%. From 0.97V to 0.94V, Voc falls. Because of enhanced light absorption, Power Conversion Efficiency (PCE) rises from 22.8% to 28.5%. By making the material thicker, the absorber layer improves light absorption and carrier production, which raises the short-circuit current density [23]. Figure 3b shows the Electron Transport Layer (ETL) layer effect on the perovskite solar cell. ETL varies from 0.01µm to 0.05µm. It shows that all the parameters are slightly increased but almost constant. The change is negligible; for this simulation, 0.05µm was gained as the optimized ETL thickness, where Open Circuit Voltage (Voc) 0.95V, Short Circuit Current (Jsc) 34.75mA/cm2, Fill Factor (FF) 85.54%, and efficiency 28.5% were achieved. This suggests that there is not much impact of ETL thickness on the perovskite solar cells (PSC's) electrical properties [24].

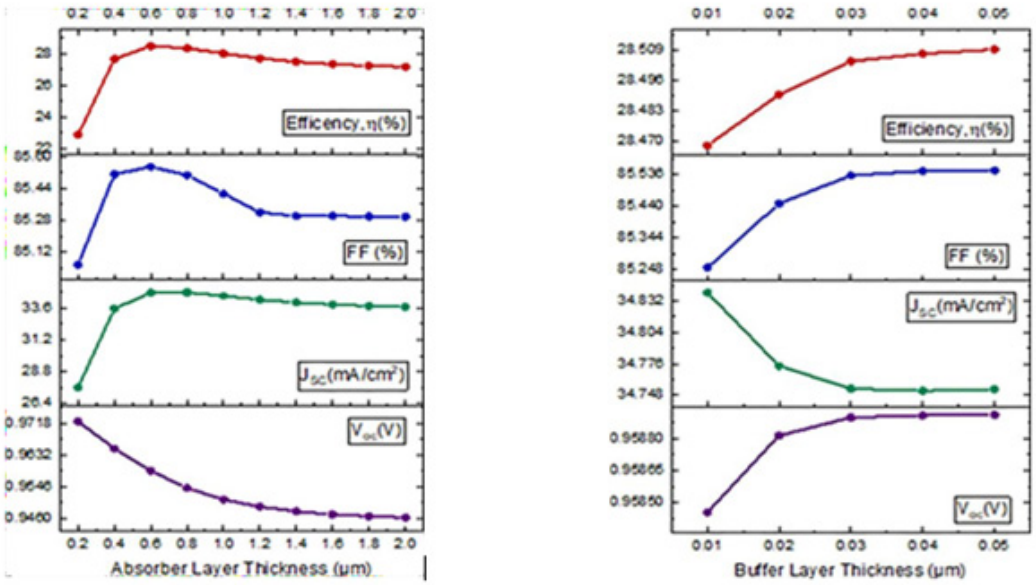

Figure 3: Effect of (a) Absorber Layer Thickness & (b) Buffer Layer Thickness on the solar cell parameters.

Effect of Series & Shunt Resistance

Figure 4a & 4b illustrates how series and shunt resistance affect the solar cell. The series resistance is changed in Figure 4a from 0.5Ωcm^{-2} to 4Ωcm^{-2}. It has been noted that, apart from Jsc, all solar cell properties decrease as series resistance rises. Fill Factor (FF) diminishes as the series resistance increases. At greater resistance values, the short circuit current decreases [25]. Here, equations 4 and 5 illustrate how series resistance affects the performance metrics.

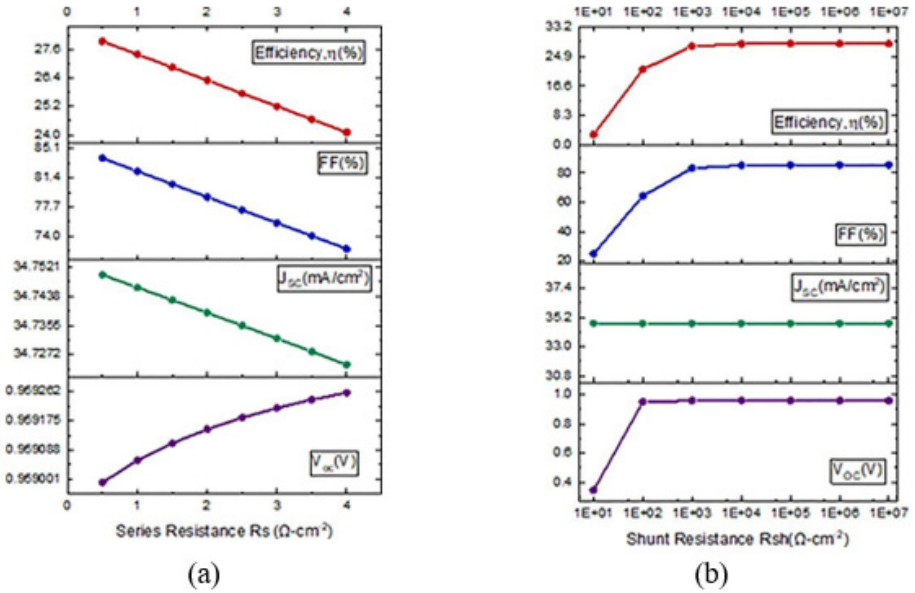

Figure 4: Effect of (a) Series Resistance & (b) Shunt Resistance on the solar cell parameters.

$$I_{SC} = I_0 \frac{70cg}{(e^{nkT-1})} \quad (4)$$

$$I_{SC} = I_l - I_o \frac{70cg}{(e^{nkT-1})} - \frac{v_{oc} + I_{scRs}}{\gamma sh} \quad (5)$$

where Ish stands for shunt resistance and IL for light-induced current. The math above makes it clear that when RS rises, the Short Circuit Current (ISC) value falls [26,27]. Figure 4b demonstrates the effect of shunt resistance on the proposed Perovskite Solar Cell (PSC). The shunt resistance is varied from 1E1Ωcm-2 to 1E7Ωcm^{-2}. As it's seen all the parameters are improved with variation. It's noticeable that there isn't much effect on short circuit current. Shunt resistance losses predominantly originate from defect state recombination; hence higher shunt resistance indicates fewer defect states [28].

Effect of Temperature & Defect Density

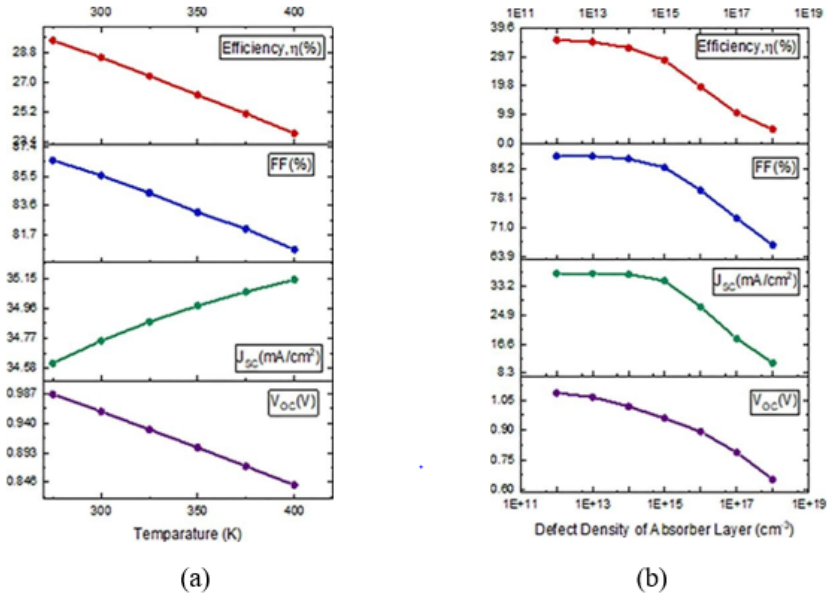

Figure 5: Effect of (a) Temperature & (b) Defect density of Absorber Layer on the solar cell parameters.

Figure 5a shows the temperature effect on the solar cell, where the temperature was adjusted from 275K to 400K. All the metrics except for short circuit current are seen to decrease gradually. This may result from a decline in efficiency brought on by the defect density in the layers rising with temperature. Temperature-related increases in deformation stress may result

in a drop in the device's efficiency [29]. Here, Open Circuit Voltage (Voc) decreases from 0.987V to 0.83V, Fill Factor (FF) 86.5% to 80.2%, and Power Conversion Efficiency (PCE) 29.3% to 23%. Because temperature alters the diffusion length, which raises the series resistance, the device's FF and efficiency are reduced [30]. For this device simulation, an optimized temperature was gained at 300K. The impact of absorber layer defect density on the solar cell is depicted in Figure 5b. In this case, the defect varies between 1E12cm^{-3} and 1E18cm^{-3}. This variation affects every parameter in this case. Power Conversion Efficiency (PCE) decreases to 5% from 36%. Short Circuit Current (Jsc) ranges from 35.6mA/cm^2 to 11mA/cm2, Fill Factor (FF) from 87.6% to 65%, and Open Circuit Voltage (Voc) from 1.1V to 0.62V. An increase in defect density causes shorter carrier lifetimes because more recombination and traps are present, making paths accessible. This lowers effective carrier mobility [31]. Defects must occur in all materials due to the possibility of achieving high efficiency at low defect concentrations [32]. For this reason, we selected the absorber layer defect density of 1E15cm^{-3}.

Quantum Efficiency & Current Density- Voltage Characteristics

Figure 6a shows the Quantum Efficiency (Q-E) vs wavelength characteristics curve. It shows the highest absorption in the wavelength range that is visible. There is a noticeable decline in Q-E in the infrared wavelength range. In this case, the absorber layer varies between 0.2 and 2µm. An optimal thickness of 0.6µm was obtained for this simulation. Figure 6a shows that as the thickness of the absorber layer increases, quantum efficiency rises at longer wavelengths. This is because there aren't enough photons inside the absorber layer to create enough electron-hole pairs [33]. Figure 6b displays the solar cell's J-V properties. In this simulation, the thickness of the absorber layer is adjusted from 0.2µm to 2µm. Here, 0.6µm was the ideal thickness for the absorber layer, resulting in an Open Circuit Voltage (Voc) of 0.95V, Short Circuit Current (Jsc) of 34.75mA/cm2, Fill Factor (FF) of 85.54%, and efficiency of 28.5%. When the absorber is thickened, the electron-hole pair is added, which raises the voltage and current [34].

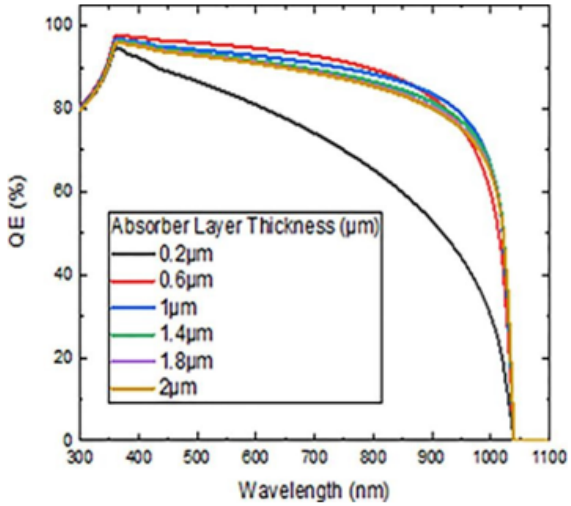

Figure 6: (a) Quantum Efficiency & (b) Current-Voltage characteristics of the PSC solar cell.

Interface Defect

Effect of ETL/ absorber and absorber/ HTL interface defect density

The impact of interface defect density on the suggested perovskite solar cell is depicted in Figure 7. This simulation changes the Electron Transport Layer (ETL/Absorber layer and the Absorber/ Hole Transport Layer (HTL) interface from 1E10cm^{-3} to 1E14cm^{-3}. Through simulation, it is found that interface fault densities significantly impact all the parameters. Low photocurrent generation and overall efficiency are caused by high defect density because it creates mid-gap trap states that serve as recombination without radiation focal points, restricting diffusion length and carrier lifetime [35]. Figure 7b shows the Absorber/ Hole Transport Layer (HTL) defect density on the proposed perovskite solar cell. High interface fault density causes efficiency to drop quickly. Defect causes recombination centers for charging carriers, which lowers efficiency and current density [36]. Because of this, an interface defect density of less than 1E11cm-3 [37] and a thickness of 0.6µm are required for the maximum efficiency (Table 2).

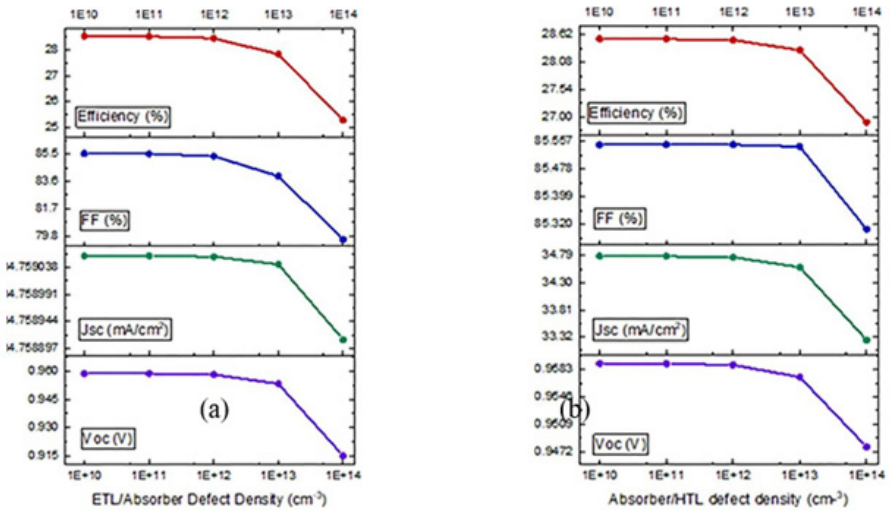

Figure 7: Effect of (a) ETL/Absorber (b) Absorber/ HTL defect density on the solar cell parameters.

Table 2: Table-2 shows the interface defect density for the device.

Interface Defect Parameters Defect Type	ETL/Absorber Neutral	HTL/Absorber Neutral
Capture cross section electrons (cm^2)	1.00E-19	1.00E-19
Capture cross section holes (cm^2)	1.00E-19	1.00E-19
Energetic distribution	Single	Single
Reference for defect energy level Et	Above the highest EV	Above the highest EV
Energy with respect to Reference (eV)	0.6	0.6
Total density (integrated over all energies) (cm^{-2})	1E10-1E14	1E10-1E14

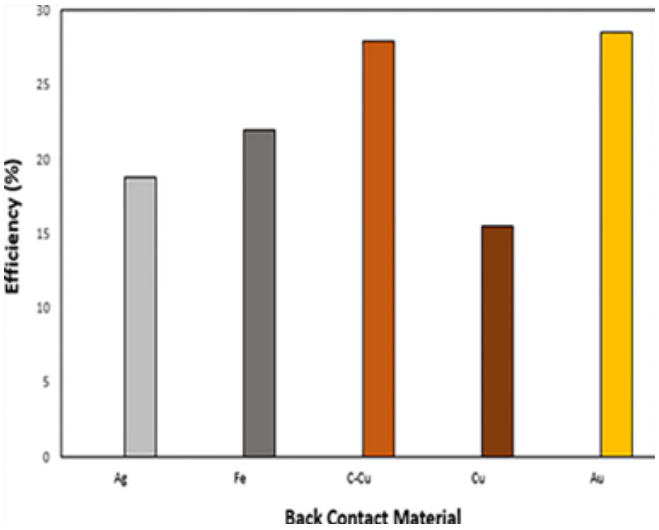

Figure 8: Different back contact materials' effects on solar cells.

Table 3: Table-3 shows metal work function for different materials.

Back Contact Metal	Ag	Fe	Au	Cu	Cu doped C
Work Function	4.7	4.8	5.3	4.6	5

Effect of Back Contact Material

The metal's quantity of energy is known as the work function or the number of photons necessary to eliminate a single electron from its surface [38]. Improved solar cell efficiencies have been associated with higher work function values [39,40]. Au and Pt are expensive metals frequently employed as back contact in solar cells (Table 3). In this work, simulations were conducted to find an appropriate, commercially accessible metal to serve as the back contact for the proposed device configuration. Figure 8 shows the impact of various materials used for back contact on the PCE [41]. The maximum efficiency that was reached in this instance was 28.5%.

Conclusion

This research studies a noble perovskite structure as ITO/ZnSe/$(CH_3NH_3)_2CuCl_4$/$SrCu_2O_2$/Au using SCAPS 1D simulation software. This study analyzes the effect of absorber layer thickness, buffer layer thickness, defect density of absorber layer, series resistance and shunt resistance to get the optimized value. Furthermore, quantum efficiency and current density-voltage characteristics were investigated for the proposed perovskite solar cell. After simulation, the optimum value of absorber layer thickness 0.6µm, total defect density Nt 1E15cm^{-3} was gained. It's observed that at 300K, the device performs at its highest level. After simulation of Voc 0.95V, Jsc 34.75mA/cm^2, FF 85.54% and efficiency 28.5% were gained as optimized values. Overall, this proposed perovskite solar cell is observed as a high-efficiency, green and stable heterojunction cell.

Acknowledgments

The authors would like to thank Dr. Marc Burgelman and his colleagues at the Department of Electronics and Information Systems (ELIS), University of Gent, Belgium, for providing the SCAPS simulation package.

References

1. Şen Z (2004) Solar energy in progress and future research trends. Progress in Energy and Combustion Science 30(4): 367-416.
2. Hattab Ml, Moudou L, Khenfouch M, Bajjou O, Chrafih Y, et al. (2021) Numerical simulation of a new heterostructure CIGS/GaSe solar cell system using SCAPS-1D software. Solar Energy 227: 13-22.
3. Litimein F, Khenata R, Bouhemadou A, Douri YA, Oman SB (2012) First-principal calculations to investigate the elastic and thermodynamic properties of $RBRh_3$ (R=Sc, Y and La) perovskite compounds. Molecular Physics 2(110): 121-128.
4. Moulai N, Ameri M, Azaz Y, Zenati A, Douri Ya, et al. (2015) Predictive study of structural, electronic, magnetic and thermodynamic properties of $XFeO_3$ (X = Ag, Zr and Ru) multiferroic materials in cubic perovskite structure: First-principles calculations. Materials Science-Poland 33(2): 402-413.
5. Reshak AH, Abu-Jafar MS, Al-Douri Y (2016) Two symmetric n-type interfaces $SrTiO_3$/$LaAlO_3$ in perovskite: Electronic properties from density functional theory. Journal of Applied Physics 119(24): 245303.
6. Bidai K, Ameri M, Amel S, Ameri Al-Douri Y, et al. (2017) First-principles calculations of pressure and temperature dependence of thermodynamic properties of anti-perovskite $BiNBa_3$ compound. Chinese Journal of Physics 55(5): 2144-2155.
7. Pal J, Manna S, Mondal A, Das S, Adarsh KV, et al. (2017) Colloidal synthesis and photophysics of $M_3Sb_2I_9$ (M=Cs and Rb) nanocrystals: Lead-free perovskites. Angew Chem Int Ed 56(45): 14187-14191.
8. Buba AD (2016) Optoelectronic properties of zinc selenide (ZnSe) thin films deposited using Chemical Bath Deposition (CBD) technique. Current Journal of Applied Science and Technology 14(3): 1-7.
9. Abdalameer NK, Mazhir SN, Aadim KA (2020) The effect of ZnSe core/shell on the properties of the window layer of the solar cell and its applications in solar energy. Energy Reports 6(6): 447-458.
10. Noman M, Shahzaib M, Jan ST, Shah SN, Khan AD (2023) 26.48% efficient and stable $FAPbI_3$ perovskite solar cells employing $SrCu_2O_2$ as hole transport layer. RCS Advances 13(3): 1892-1905.
11. Nie X, Wei SH, Zhang SB (2002) First-principles study of transparent p-type conductive $SrCu_2O_2$ and related compounds. Physical Review B 65(7): 075111.
12. Shasti M, Mortezaali A (2019) Numerical study of Cu_2O, $SrCu_2O_2$, and $CuAlO_2$ as hole-transport materials for application in perovskite solar cells. Physica. Status Solidi A 216(18): 1900337.
13. Bandara J, Yasomanee JP (2006) P-type oxide semiconductors as hole collectors in dye-sensitized solid-state solar cells. Semicond Sci Technol 22(2): 20.
14. Zhao Y, Dong W, Fang X, Zhou Y, Meng G, et al. (2012) P-type Ca doped $SrCu_2O_2$ thin film: Synthesis, optical property and photovoltaic application. Journal of Alloys and Compounds 513: 50-54.
15. Valiente R, Elseman AM, Rodríguezet F (2020) Copper-substituted lead perovskite materials constructed with different halides for working $(CH_3NH_3)_2CuX_4$-based perovskite solar cells from experimental and theoretical view. ACS Appl Mater Interfaces 12(34): 37807-37810.
16. Liu X, Wang L, Tong Y (2020) Optoelectronic properties of ultrathin indium tin oxide films: A first-principal study. Crystals 11(1): 30.
17. Burgelman M, Nollet P, Degrave S (2000) Modeling polycrystalline semiconductor solar cells. Thin Solid Films 361: 527-532.
18. Biswas SK, Mim MK, Ahmed MM (2023) Design and simulation of an environment-friendly ZrS_2/$CuInS_2$ thin film solar cell using scaps 1D software. Advances in Materials Science and Engineering.
19. Kumar A, Sharma P (2023) Transfer matrix method-based efficiency enhancement of lead-free $Cs_3Sb_2Br_9$ perovskite solar cell. Solar Energy 259: 63-71.
20. Prasanna JL, Goel E, Kumar A (2023) Numerical investigation of $MAPbI_3$ perovskite solar cells for performance limiting parameters. Optical Quantum Electron 55: 610.
21. Burgelman M, Decock K, Niemegeers A, Verschraegen J, Degrave S (2016) SCAPS Manual.
22. Dastan D, Mohammed MK, Mousoi AK, Kumar A, Salih SQ, et al. (2023) Insights into the photovoltaic properties of indium sulfide as an electron transport material in perovskite solar cells. Sci Rep 13(1): 9076.
23. Bakirci K (2012) The effect of absorber layer thickness on the performance of solar cells. Renew Energy 37(1): 67-70.
24. Sarker K, Sumon S, Orthe F, Biswas SK, Ahmed M (2023) Numerical simulation of high efficiency environment friendly $CuBi_2O_4$-based thin-film solar cell using SCAPS-1D. Internal Journal of Photoenergy.

25. Chakraborty K, Choudhury MG, Paul S (2019) Numerical study of Cs_2TiX_6 (X = Br^-, I^-, F^- and Cl^-) based perovskite solar cell using SCAPS-1D device simulation. Solar Energy 194: 886-892.

26. Heriche H, Rouabah Z, Bouarissa N (2017) New ultra-thin CIGS structure solar cells using SCAPS simulation program. International Journal of Hydrogen Energy 42(15): 9524-9532.

27. Jeon JN, Noh JH, Yang WS, Kim YC, Ryu S, et al. (2015) Compositional engineering of perovskite materials for high-performance solar cells. Nature 517(7535): 476-480.

28. Naureen, Sadanand, Lohia P, Dwivedi DK, Ameen S (2022) A comparative study of quantum dot solar cell with two different ETLs of WS_2 and IGZO using SCAPS-1D simulator. Solar 2(3): 341-353.

29. Srivastava P, Sadanand, Shambhavi R, Lohia P, Dwivedi DK, et al. (2022) Theoretical study of perovskite solar cell for enhancement of device performance using SCAPS-1D. Physica Scripta 97(12): 125004.

30. Biswas SK, Sumon S, Sarker K, Orthe F, Ahmed M (2023) A Numerical Approach to Analysis of an environment-friendly Sn-based perovskite solar cell with SnO_2 buffer layer using SCAPS-1D. Advances Materials Science and Engineering.

31. Mishra S, Bhargava K, Deb D (2019) Numerical simulation of Potential Induced Degradation (PID) in different thin-film solar cells using SCAPS-1D. Solar Energy 188: 353-360.

32. Karthick S, Velumani S, Bouclé J (2020) Experimental and SCAPS simulated formamidine perovskite solar cells: A comparison of device performance. Solar Energy 205: 349-357.

33. Sunny A, Rahman S, Mishty MK, Ahmed SR (2021) Numerical study of high performance HTL-free $CH_3NH_3SnI_3$-based perovskite solar cell by SCAPS-1D. AIP Advances 11(6): 065102.

34. Li H, Ali W, Wang Z, Mideksa MF, Wang F, et al. (2019) Enhancing hot-electron generation and transfer from metal to semiconductor in a plasmonic absorber. Nano Energy 63: 103873.

35. Mim MK, Biswas SK (2025) Performance analysis of Sr_3SbI_3-based perovskite solar cell using SCAPS-1D Software. Advances Materials Science and Engineering.

36. Khatoon S, Chakraborty V, Satish K, Diwakar S, Jyotsna S, et al. (2023) Simulation study of $CsPbI_xBr_{1-x}$ and $MAPbI_3$ heterojunction solar cell using SCAPS-1D. Solar Energy 254: 137-157.

37. Chowdhury MS, Shahahmadi SA, Chelvanathanet P, Tiong SK, Amin N, et al. (2020) Effect of deep-level defect density of the absorber layer and n/i interface in perovskite solar cells by SCAPS-1D. Results in Physics 16:102839.

38. Anwar F, Afrin S, Satter SS, Rafee M (2017) Simulation and performance study of nanowire CdS/CdTe solar cell. International Journal of Renewable Energy Research 7(2): 885-893.

39. Derry GN, Kern ME, Worth EH (2015) Recommended values of clean metal surface work functions. Journal of Vacuum Science and Technology 33: 060801.

40. Thahab SM, Hassan HA, Hassan Z (2006) Effects of metal work function and operating temperatures on the electrical properties of contacts to n-type GaN. IEEE International Conference on Semiconductor Electronics (ICSE): 816-819.

41. Ganem HT, Saleh AN (2021) Enhancement of the efficiency of the CZTS/Cds/Zno/ITO solar cell by back reflection and buffer layers using SCAPS-1D. Iraqi Journal of Science 6: 1144-1157.